Human Molecular Genetics, 2016, Vol. 25, No. 11 2158–2167

doi: 10.1093/hmg/ddw082
Advance Access Publication Date: 22 March 2016
Original Article

ORIGINAL ARTICLE

Heterozygous *KIDINS220/ARMS* nonsense variants cause spastic paraplegia, intellectual disability, nystagmus, and obesity

Dragana J. Josifova[1,†], Glen R. Monroe[2,3,†], Federico Tessadori[2,3,4,†], Esther de Graaff[5], Bert van der Zwaag[2], Sarju G. Mehta[6], The DDD Study[7], Magdalena Harakalova[2], Karen J. Duran[2,3], Sanne M.C. Savelberg[2,3], Isaäc J. Nijman[2,3], Heinz Jungbluth[8,9,10], Casper C. Hoogenraad[5], Jeroen Bakkers[4,11], Nine V. Knoers[2,3], Helen V. Firth[6,7], Philip L. Beales[12], Gijs van Haaften[2,3,‡] and Mieke M. van Haelst[2,*,‡]

[1]Department of Clinical Genetics, Guys' and St. Thomas' Hospital, London SE1 7EH, UK, [2]Department of Genetics, [3]Center for Molecular Medicine, University Medical Center Utrecht, Utrecht 3584 CX, The Netherlands, [4]Hubrecht Institute-KNAW and University Medical Center Utrecht, Utrecht 3584 CT, The Netherlands, [5]Division of Cell Biology, Faculty of Science, University of Utrecht, Utrecht 3584 CH, The Netherlands, [6]Department of Clinical Genetics, Cambridge University Hospitals NHS Foundation Trust, Addenbrooke's Hospital, Cambridge CB2 0QQ, UK, [7]Wellcome Trust Sanger Institute, Wellcome Trust Genome Campus, Hinxton, Cambridgeshire CB10 1RQ, UK, [8]Department of Paediatric Neurology, Evelina Children's Hospital, Guy's & St Thomas' Hospital NHS Foundation Trust, London SE1 7EH, UK, [9]Randall Division of Cell and Molecular Biophysics, Muscle Signalling Section, and [10]Department of Basic and Clinical Neuroscience, IoPPN, King's College, London WC2R 2LS, UK, [11]Department of Medical Physiology, University Medical Center Utrecht, Utrecht 3584 CX, The Netherlands and [12]Genetics and Genomics Medicine Program, UCL Institute of Child Health, London WC1N 1EH, UK

*To whom correspondence should be addressed at: Lundlaan 6, 3581EA, Utrecht, The Netherlands. Tel: +31 887553800; Email: m.vanhaelst@umcutrecht.nl

Abstract

We identified *de novo* nonsense variants in *KIDINS220/ARMS* in three unrelated patients with spastic paraplegia, intellectual disability, nystagmus, and obesity (SINO). KIDINS220 is an essential scaffold protein coordinating neurotrophin signal pathways in neurites and is spatially and temporally regulated in the brain. Molecular analysis of patients' variants confirmed expression and translation of truncated transcripts similar to recently characterized alternative terminal exon

[†]The authors wish it to be known that, in their opinion, the first three authors should be regarded as joint First Authors.
[‡]The authors wish it to be known that, in their opinion, the last two authors should be regarded as joint Last Authors.
Received: December 11, 2015. **Revised:** March 10, 2016. **Accepted:** March 10, 2016

splice isoforms of *KIDINS220*. *KIDINS220* undergoes extensive alternative splicing in specific neuronal populations and developmental time points, reflecting its complex role in neuronal maturation. In mice and humans, *KIDINS220* is alternative spliced in the middle region as well as in the last exon. These full-length and *KIDINS220* splice variants occur at precise moments in cortical, hippocampal, and motor neuron development, with splice variants similar to the variants seen in our patients and lacking the last exon of *KIDINS220* occurring in adult rather than in embryonic brain. We conducted tissue-specific expression studies in zebrafish that resulted in spasms, confirming a functional link with disruption of the KIDINS220 levels in developing neurites. This work reveals a crucial physiological role of *KIDINS220* in development and provides insight into how perturbation of the complex interplay of *KIDINS220* isoforms and their relative expression can affect neuron control and human metabolism. Altogether, we here show that *de novo* protein-truncating *KIDINS220* variants cause a new syndrome, SINO. This is the first report of *KIDINS220* variants causing a human disease.

Introduction

Next Generation Sequencing (NGS) techniques provide a time and cost-efficient method to identify novel genes. We used this approach to investigate two patients presenting with an apparently unique combination of features, including obesity, spastic paraplegia, intellectual disability, nystagmus and macrocephaly and identified different, *de novo*, heterozygous, nonsense variants in *KIDINS220* in each patient. A third patient with similar features was ascertained through DECIPHER (decipher.sanger.ac.uk) after the DDD study shared a *de novo* candidate variant identified by trio exome analysis (1,2).

KIDINS220 (Kinase D interacting substrate of 220 kDa), also known as ARMS (Ankyrin Repeat-rich Membrane Spanning), is a conserved scaffold protein that controls axonal and dendritic maturation (3,4). The spatiotemporal expression of different KIDINS220 isoforms is finely tuned in the mammalian brain, and knock-out *Kidins220* animals show developmental central nervous system anomalies (5–7). Recently, it was shown that distinctive neuronal populations express different KIDINS220 splice isoforms at specific times during development, including newly characterized alternative terminal exon (ATE) splice isoforms (8). The expression of the complete range of these isoforms, with the corresponding domains for thus far poorly characterized interaction partners, may be crucial for proper neuronal development. We show here that our patients' variants result in truncated isoforms of KIDINS220 similar to an ATE splice isoform expressed mainly during adulthood. Our patients' neurological phenotype may be caused by disruption of full-length KIDINS220 splice isoform repertoire expression and lack of essential interaction domains that are necessary during embryonic development of the neural network. We further show that perturbation of *KIDINS220* levels causes a spasticity phenotype in zebrafish. We therefore suggest that *KIDINS220* variants cause a new syndrome characterized by spastic paraplegia, intellectual disability, nystagmus and obesity (SINO syndrome).

Results

De novo KIDINS220 variants are implicated in patients with a unique phenotype of SINO

We performed NGS analysis in three unrelated patients with SINO (Fig. 1 and Table 1, Supplementary Materials).

Two patients were sequenced for a targeted gene panel of 582 genes to investigate the suspected genetic cause of syndromic and non-syndromic obesity (OBESITOME, UMC Utrecht, The Netherlands) (Supplementary Material, Table S1). We identified heterozygous *KIDINS220* variants, NM_020738.2:c.4050G > A, p.(Trp1350*) and NM_020738.2:c.4096C > T, p.(Gln1366*), in patient 1 and 2, respectively. Both variants result in a premature stop codon. Their *de novo* occurrence was confirmed by Sanger sequencing of both patients and their parents. There were no further *de novo* variants in other shared genes on the OBESITOME panel. Independently, whole exome sequencing on patient 3 revealed a heterozygous *de novo* insertion of an A nucleotide, NM_020738.2:c.4520dup, resulting in a frameshift and predicted premature truncation of the protein p.(Leu1507Phefs*4) (1,2) (Fig. 2A and B).

Variant *KIDINS220* RNA expression results in truncated KIDINS220 in patient fibroblasts and HEK293T cells

All variants identified here fall within the last two exons of the gene (Fig. 2A and B). Sanger sequencing on fibroblast cDNA from patient 1 showed that variant c.4050G > A resulted in proper mRNA expression (Fig. 2C). This result was confirmed by Quantitative PCR, with the relative expression of *KIDINS220* before and after the variant c.4050G > A equal in patient fibroblast cDNA compared with control fibroblast cDNA, indicating that the shortened transcript escaped nonsense-mediated decay (NMD) (data not shown). The mammalian NMD pathway is unable to recognize premature termination codons in the last exon and the last ~55 bp of the penultimate exon (9). Shortened mRNA transcripts that escape NMD are translated into truncated protein products possibly lacking important C-terminal domains. Variants in the penultimate exon resulting in premature stop codons that escape NMD are reported in other syndromes, e.g. autosomal dominant Robinow syndrome (10). Furthermore, we used cDNA sequencing to assess known alternative splicing of exon 25 and exon 26 in the middle region of KIDINS220, which has not yet been determined in fibroblast cells. Patient and control cDNA sequencing of the region flanking and containing exons 25 and 26 revealed that fibroblasts from both our patient 1 and control express *KIDINS220* with exon 26 removed by alternative splicing (GenBank accession no. KJ812120), indicating that exon 26 is removed in all fibroblast cells (data not shown).

We analyzed total protein extract of fibroblasts of patient 1 by Western blot analysis and detected a 150 kDa band in addition to the 220 kDa wild-type KIDINS220 band, confirming expression of the truncated, Trp1350* protein (Fig. 2D). The variants of patient 1 and 2 were also overexpressed separately in HEK293T cells to visualize the size of the truncated protein products, using human isoform containing both exons 25 and 26 (GenBank accession no. KJ812119) (8). The presence of a 150 kDa protein coinciding with the p.(Trp1350*) variant of patient 1 and a 167 kDa protein coinciding with the p.(Gln1366*) variant of patient 2 were

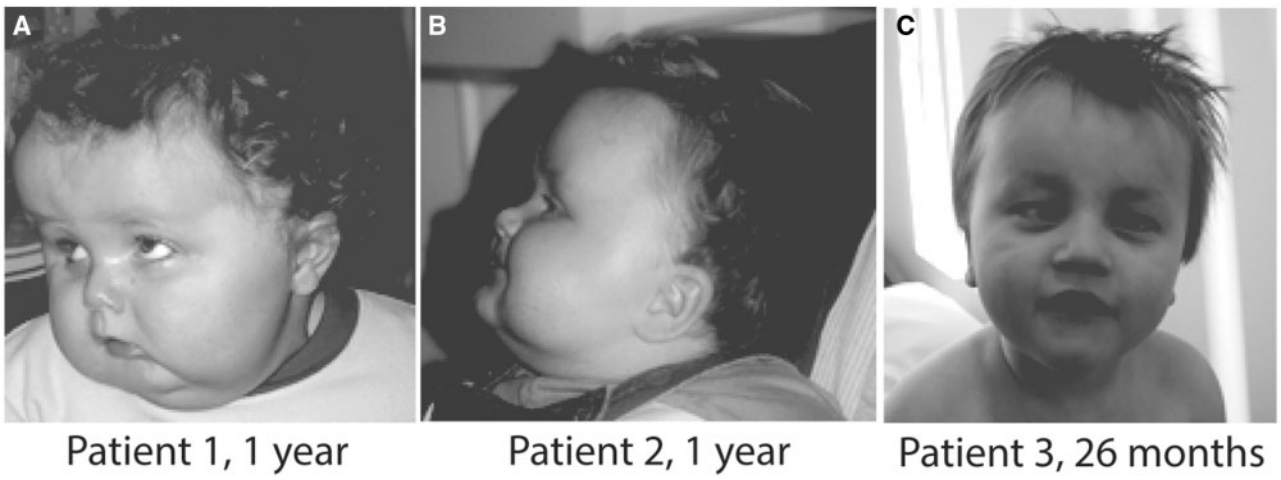

Figure 1. Clinical features of patients. Note obesity, macrocephaly, brachycephaly and eye abnormalities.

Table 1. Clinical phenotype of the three patients with *KIDINS220 de novo* variants

	Patient 1	Patient 2	Patient 3
Prenatal Scan	Dilatation of lateral ventricles	Dilatation of lateral ventricles	Dilatation of lateral ventricles
Polyhidramnious	−	+	?
Gestational age (weeks)	38	40	41
Weight (birth)	2.26 kg (second centile)	3.65 kg (75th centile)	3.28 (50th centile)
Weight (infancy)	>99.6th centile	99.6th centile	98th centile
Weight (puberty)	>99.6th centile	>99.6th centile	Overweight
Height (infancy)	91–98th centile	91st centile	75th centile
Height (puberty)	91st centile	91st centile	?
OFC (birth)	25–50th centile	?	?
OFC (infancy)	≫99.6th centile	99.6th centile	98th centile
OFC (puberty)	99.6th centile	>99.6th centile	25–50th centile
Feeding pattern	Nl	Nl	Nl
Dysmorphic features	Brachyplagiocephaly Bossed forehead Deep set eyes	Brachyplagiocephaly Prominent forehead Deep-set eyes Crowded teeth	Brachyplagiocephaly Prominent forehead
Vision	Reduced acuity Hypermetropia Astigmatism	Squint Hypermetropia Astigmatism	Squint Hypermetropia Esotropia
Nystagmus	+	+	+
ERG	Nl	?	?
VEP	Post retinal dysfunction	?	?
Development	Delayed	Delayed	Delayed
Neurology	Axial hypotonia Spastic paraplegia	Spastic paraplegia	Spastic paraplegia
Brain MRI	Dilated lateral and third ventricles Normal fourth ventricle Reduced white matter bulk Mild delay in myelination Mild generalized atrophy	Dilated third and lateral ventricles Normal fourth ventricle Reduced white matter bulk Mild generalized atrophy	Dilated lateral ventricles High riding third ventricle Partial agenesis of corpus callosum
Bone age	?	Slightly delayed	?
Eating habits	Nl	Nl	Nl
Development	Moderate global delay	Moderate global delay	Moderate global delay

Nl, normal, +, present, −, absent, ?, not reported; OFC, occipito frontal circumference; ERG, electroretinogram; VEP, visual evoked potential.

detected by Western blot. Only wild-type 220 kDa protein was identified in HEK293T extracts overexpressing the wild-type KIDINS220 (Fig. 2E). The KIDINS220 protein product of these variants is strikingly similar to that produced by ATE splicing in mouse and humans (ATE C2) (Fig. 2B) (8).

Motor neuron specific expression of KIDINS220 variants induces spasms in zebrafish

Zebrafish is a powerful, versatile vertebrate model to study human motor neuron diseases (11,12). By using the Gal4/UAS approach (13,14) we achieved motor neuron-specific expression of

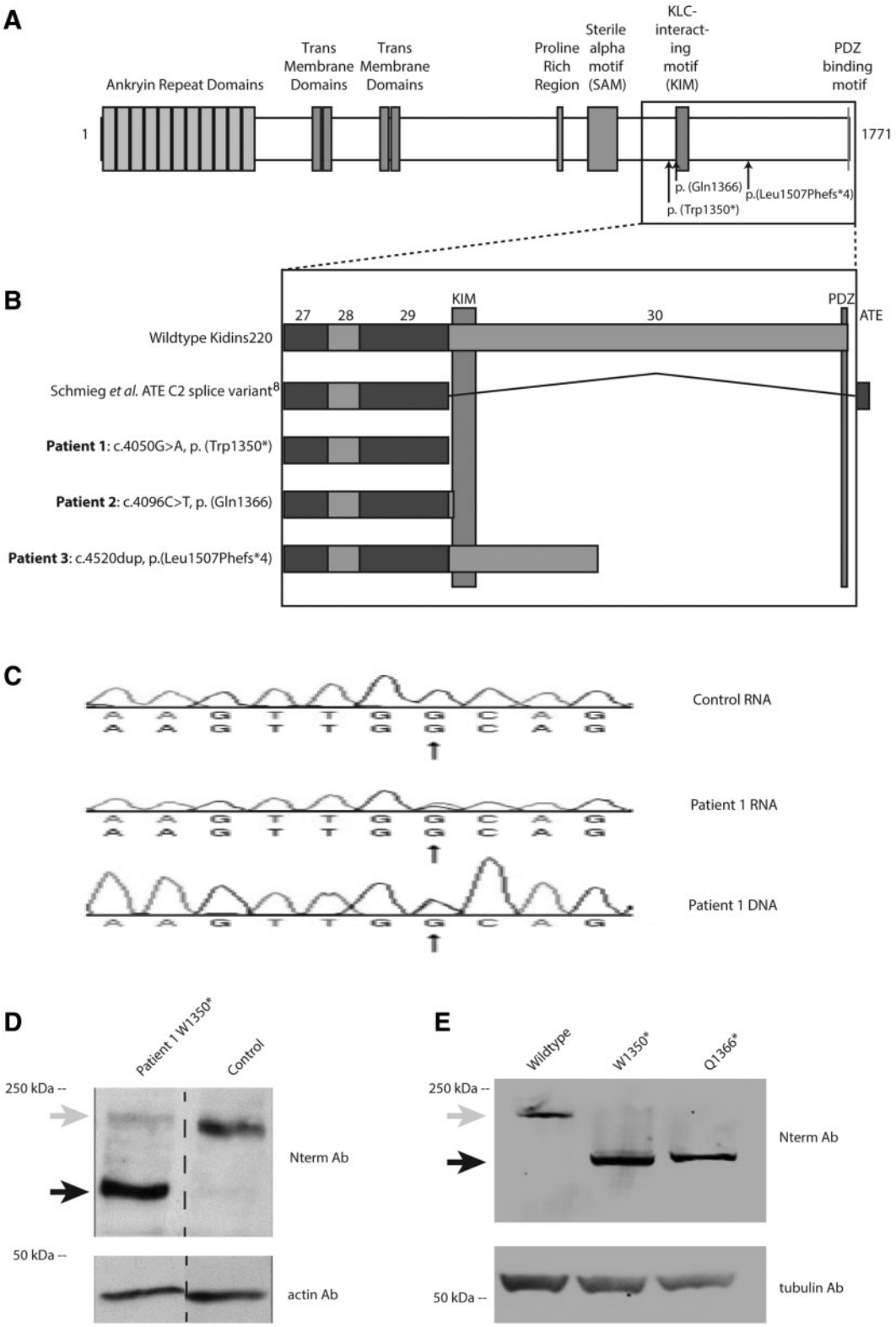

Figure 2. *De novo* dominant nonsense variants in *KIDINS220*. **(A)** Variants p.(Trp1350*) and p.(Gln1366*) result in truncated protein without the full KIM domain, and p.(Leu1507Phefs*4) results in a slightly longer protein containing the full KIM domain. **(B)** Comparison of the wild-type *KIDINS220* exonic structure versus an alternate terminal ending splice variant described by Schmieg *et al.* (8) and the three patients described in this study **(C)** *KIDINS220* cDNA sequencing verifies that there is no mRNA NMD in patient 1. Western blot analysis of **(D)** total extracts from patient 1 versus a control fibroblast and **(E)** total HEK293T extracts expressing wild-type and variant (Trp1350* and Gln1366*) forms of KIDINS220. Expression of KIDINS220 was tested with antibodies against the N-terminal part of KIDINS220 (Nterm Ab). The truncated protein products caused by KIDINS220 variants are indicated with a black arrow and the expected full-length wild-type protein product by a grey arrow. Anti-actin was used as a loading control for the fibroblasts and anti-tubulin for the HEK293T cells.

human *KIDINS220* variants in zebrafish embryos and analyzed their effect *in vivo*. Transgenic tg(Isl1BAC:GalFF) fish used here constitutively express Gal4 in motor neurons; when DNA constructs containing an upstream activation sequence (UAS) driving transcription are supplemented by microinjection, mosaic larvae are obtained in which Gal4 binds to the UAS sequence to express *KIDINS220* solely in motor neurons. Embryos tg(Isl1BAC:GalFF) microinjected with UAS:KIDINS220 wild-type or variant p.(Trp1350*) displayed spasms in the trunk at 5 days post fertilization (dpf), confirming a functional link between spasticity and disruption of KIDINS220 levels and/or function (Fig. 3). This was slightly more evident in embryos expressing the mutant *KIDINS220*. Representative recordings of the spasm phenotypes can be found in the Supplementary Material online.

Kidins220 variants do not result in different cellular localizations in Neuro-2A cells

During differentiation, KIDINS220 is transported to the neurite tips of PC12 neuronal cells, a process that is altered in KIDINS220 isoforms with an ATE (4,8). We examined the cellular location of wild-type and truncated KIDINS220 in Neuro-2A cells, a cell line where KIDINS220 is endogenously expressed, albeit at lower levels than in PC12 cells (4). Following cotransfection of HA-tagged wild-type or p.(Gln1366*) *KIDINS220* as well as a mCherry reporter, Neuro-2A cells were differentiated with retinoic acid for a total of 5 days. Fixation was performed at day 5 and immunofluorescence performed with an anti-HA antibody. Differentiated cells expressing wild-type or p.(Gln1366*) exhibited localization of KIDINS220 throughout the entire cell body, as well as in the neurite tips. There was no difference in the cellular localization of the wild-type or variants (Fig. 4).

Discussion

KIDINS220 controls axonal and dendritic maturation in the developing mammalian brain, and is integral to the branching, stabilization and complexity of cortical and hippocampal dendrites (3,4,7). The cytoplasmic N-terminus contains 11 ankyrin repeats. There are four transmembrane segments in the central part of the molecule (15). The C-terminal tail, also exposed to the cytoplasm, contains several protein–protein interacting domains: a proline-rich domain, Sterile Alpha Motif (SAM), Kinesin Light Chain (KLC)—Interactive Motif (KIM) and PDZ-binding motif (3,16). These domains enable the recruitment of cell-specific adaptors and effectors to activated Tropomyosin receptor Kinases (TrK) and are involved in functional interactions with other receptors such as the Glutamate, Ephrin and Vascular Endothelial Growth Factor receptors (6,17). The KIM domain mediates intracellular trafficking of KIDINS220 through direct binding to KCL-1 and -2 and is important for a correct response to neurotrophic stimuli (16,18). Expression of *KIDINS220* is developmentally regulated and differential splicing occurs in specific tissues such as the brain, heart, and skeletal muscle. The alternative splicing is complex and developmental occurrence of *KIDINS220* splice isoforms with the middle region and/or last exon removed varies in cortical, hippocampal and motor neurons (8). Schmieg *et al.* (8) demonstrated in mice that *KIDINS220* with exon 30 included is expressed in embryonic tissue; in contrast, a similar *KIDINS220* splice variant lacking exon 30 is present solely in adult tissue. Motor neurons exhibited the highest variety of alternative splicing in the middle region, but did not exhibit any ATE splicing at any time during development. Our patients' variants result in isoforms similar to KIDINS220 splice variants with ATE splicing. The constitutive expression of truncated isoforms similar to ATE splice isoforms that are not usually expressed in the developing embryo or present in motor neurons, may perturb the complex splice regulation necessary for proper neurite development and result in the phenotype seen in our patients.

In this manuscript we show that *KIDINS220* nonsense variants are causal for a characteristic phenotype most likely due to disruption of the repertoire of splice isoforms available for developing neuronal populations. Interference in the delicate balance of KIDINS220 isoform expression in the neurite tips will impede the various Neurotrophin, Glutamate, Ephrin and Vascular Endothelial Growth Factor receptor associations required for correct neuronal network development. The C-terminal region of KIDINS220 contains the KIM and PDZ domains that are required for protein interactions and transport. Lack of the KIM domain and its interaction with KCL-1 subunit KIF5A (Kinesin Family Member 5A) impairs protein transport to newly formed neurite tips (16). Similarly, absence of a PDZ domain will interfere with the interaction of KIDINS220 with SNX27 (Sorting Nexin Family Member 27), an important protein for transport to the plasma membrane (19). We here show in *KIDINS220* transfected Neuro-2a cells, both wild-type and KIDINS220 variant p.(Gln1366*) successfully localized to the differentiating neurite tips, indicating an alternate as-of-yet undetermined molecular pathology due to the variants seen in our patients.

Studies of Kidins220 during zebrafish and Xenopus Laevis embryogenesis showed dynamic expression in the nervous system including the hypothalamus, eye, branchial arches, heart and somites, partly correlating with the anomalies observed in our patients (20,21). Mice completely lacking Kidins220 are not viable (5–7). The extensive neuronal cell death in the brain of mutant embryos results in abnormal ventricle enlargement. This observation appears concordant with the pre and post natal ventriculomegaly observed in our patients. Heterozygous mice display defects in dendritic growth and branching, indicating the role of Kidins220 in Brain-Derived Neurotrophic Factor (BDNF)-induced dendritic development (6,7,22). Although the heterozygous and wild-type mice have, at several age time points, comparable total Kidins220 protein levels in the brain, it seems likely that the temporal balance between Kidins220 isoforms in the brain is crucial for correct neural development (5). Structural cardiac anomalies and defects of the vascular and immune system were also observed in *Kidins220* −/− embryos (5,6), but are not seen in any of our patients, possibly due to different isoforms being required for normal heart and brain development (8).

Zebrafish is an excellent model for human motor neuron disorders (11). Motor neuron-specific expression in zebrafish using the wild-type or variant p.(Trp1350*) KIDINS220 resulted in spasms. The observed difference in the induction of spasms in zebrafish embryos expressing the wild-type or p.(Trp1350*) truncated KIDINS220 may reflect the complex regulation of KIDINS220 tissue-specific splicing and expression. More conclusively, disruption of *KIDINS220* expression levels in motor neurons functionally links *KIDINS220* deregulation to nervous system impairment. The specific features in our zebrafish model, in particular the presence of spasms that are not observed in affected humans, confirm the effects of KIDINS220 perturbation on neuronal function but are also likely to reflect anatomical differences in the central nervous system between zebrafish and humans. Specifically, the absence of corticospinal and rubrospinal tracts in zebrafish results in the replication of human lower motor neuron disorders more faithfully than

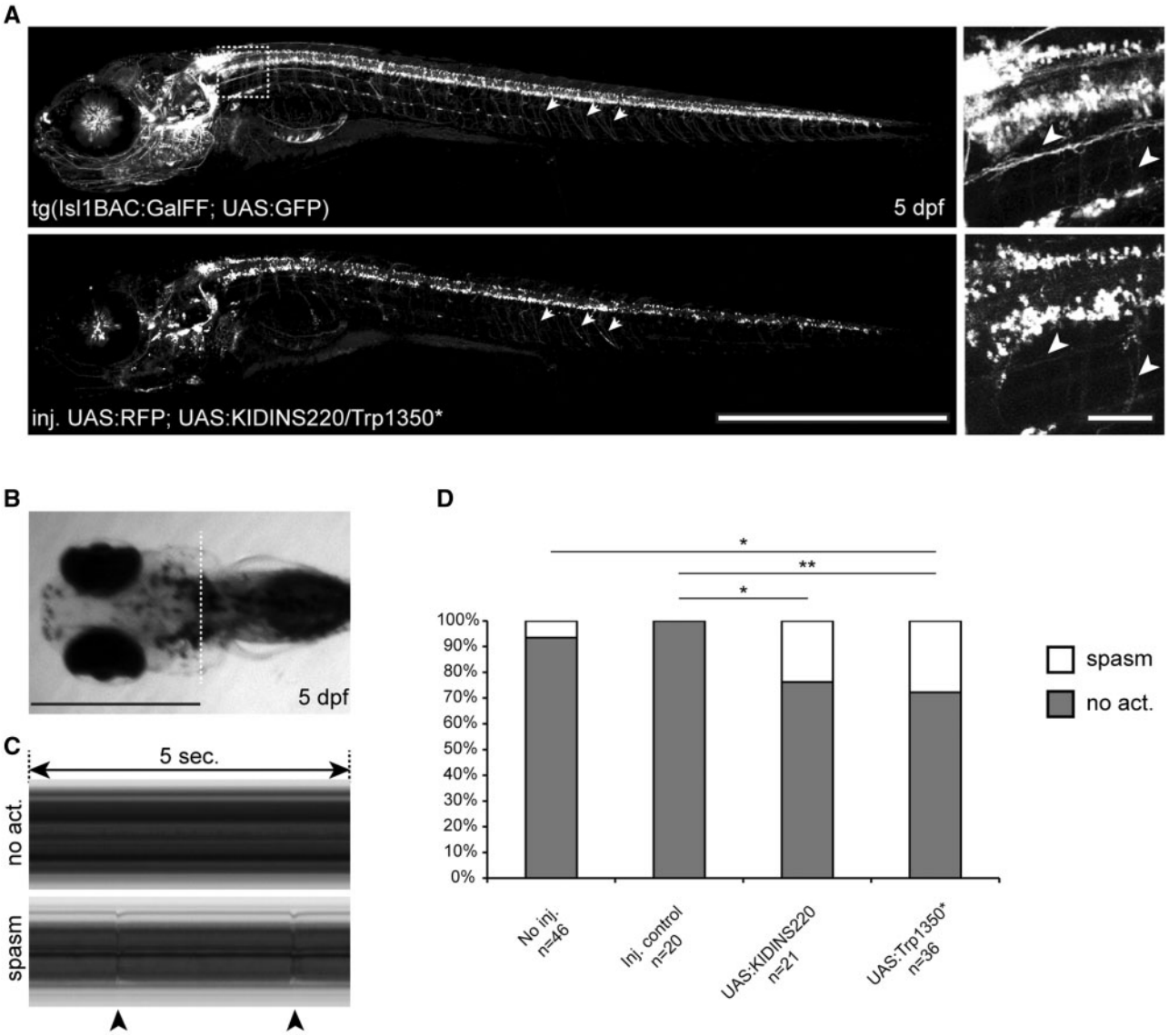

Figure 3. Effect of KIDINS220 and Trp1350* expression in zebrafish embryo motor neurons. **(A)** Tissue-specific expression of KIDINS220 variants in 5 dpf zebrafish embryos was achieved by microinjection of UAS:KIDINS220 and UAS:Trp1350* DNA in tg(Isl1BAC:GalFF; UAS:GFP) embryos (upper panel). A DNA UAS:RFP construct was co-injected (lower panel) to evaluate the efficiency of the microinjections. White arrowheads: axonic extensions of the motor neurons. **(B)** 5 dpf zebrafish embryo (ventral view; anterior is left). White dotted line: position of kymographs presented in C. **(C)** Visualization of spastic activity on thoracic kymographs. Representative kymographs of embryos showing no spastic activity (upper panel, no act.) and spastic activity (lower panel, spasm). Black arrowheads point at spastic events as visualized on the kymograph. Representative recordings are available as supplementary Material files. **(D)** Quantification of spastic events in the different conditions of the study. Expression of KIDINS220 wt and Trp1350* in motor neurons results in increased spastic activity. No act., No spastic activity. $^{*}P < 0.05$; $^{**}P < 0.01$; Fisher's exact test. Scale bars: 1 mm in A (left panels), B; 50 microns in A (right panels).

human upper motor neuron disorders on the phenotypical level. KIDINS220 is expressed in cortical and hippocampal neurons, encompassing the upper motor neuron system, and as such this dysfunction can be classified as an upper motor neuron disorder. Nonetheless, zebrafish have provided a suitable partial model for insights into the molecular and genetic mechanisms of other upper motor neuron disorders, such as hereditary spastic paraplegias (24–26).

The pathophysiology of obesity is difficult to explain. KIDINS220 is known to act as a downstream substrate for protein kinase D and mediates multiple receptors signaling including BDNF and other neurotrophins. Since neurotrophins have been implicated in the molecular and cellular processes underlying body weight regulation, disruption of this finely tuned TrK pathway could possibly explain the obesity phenotype in these patients (27,28). Increased expression of *KIDINS220* has been linked with perturbation of TrkA/p75 neurotrophin receptor complex association and overexpression of the differently spliced *KIDINS220* ATE C2 leads to a substantial increase in TrkA expression (8,23). Further research is needed to provide insight into this interaction.

Not every loss-of-function variant in the last exon of *KIDINS220* causes the phenotype observed in our patients as illustrated by the presence of three *KIDINS220* variants that are present heterozygously in five healthy individuals in the Exome Aggregation Consortium (ExAC) database (ExAC, Cambridge, MA (URL: http://exac.broadinstitute.org, last accessed September 2015). These variants, resulting in p.Glu1530Ter, p.Arg1736Ter and

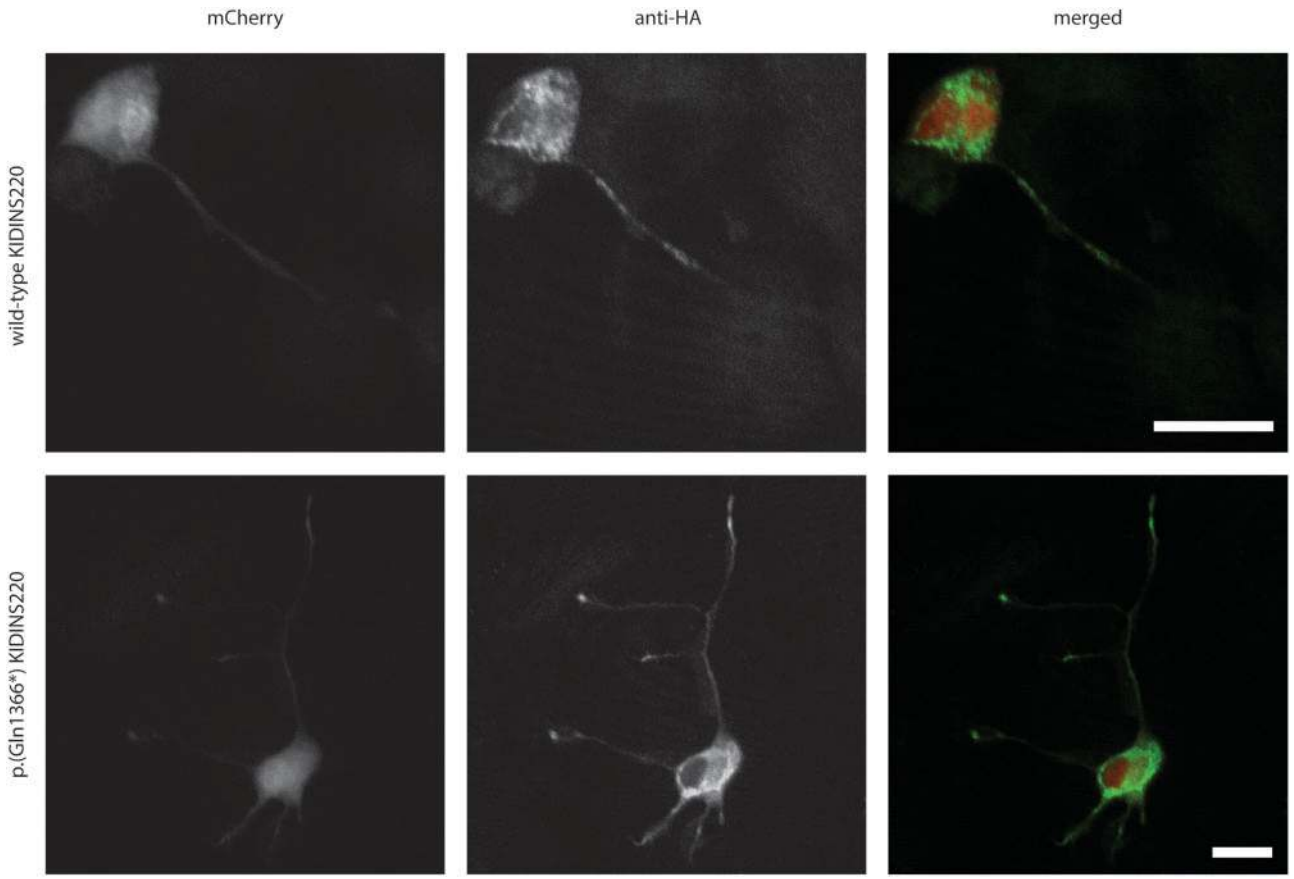

Figure 4. Kidins220 truncated variant is able to localize to neurite tips in Neuro-2A cells. Representative image of transfected KIDINS220 wild-type and variant p.(Gln1366*) in differentiated Neuro-2A cells. Immunofluorescence of cotransfected mCherry (red), anti-HA-tagged wild-type or p.(Gln1366*) KIDINS220 (green) show that the truncated KIDINS220 variant is transported to developing neurite tips. Scale bar = 20 microns

p.Ser1740Ter, are shortly after the variant in our patient 3, pointing to a specific effect of the variants presented in this study.

Our patients manifest similarities with MOMO Syndrome (**M**acrosomia, **O**besity, **M**acrocephaly and **O**cular abnormalities; OMIM 157980); however, prenatal ventricular dilatation and spastic paraplegia are not features of this condition. *KIDINS220* Sanger sequencing of 10 MOMO patients did not yield any variants. We therefore suggest that our patients have a distinct syndrome characterized by SINO.

In conclusion, we show here that *de novo* heterozygous nonsense *KIDINS220* variants cause SINO syndrome. This is the first report of *KIDINS220* variants causing a human disease. Future research might provide more insights in the role of *KIDINS220* in the pathogenesis of spastic paraplegia and obesity.

Materials and Methods

Clinical Features

The clinical features of the three patients are summarized in Figure 1 and Table 1 and case reports can be found in Supplementary Materials.

NGS and analytical pipeline

NGS on patients 1 and 2 was performed with fragment libraries prepared and enriched for the genomic regions of interest using a 1M custom OBESITOME microarray (Agilent Technologies, Santa Clara, CA, USA) as previously described in (29,30). The OBESITOME contained 582 obesity-related genes, with the genes selected on presumed obesity relevance from several databases, pathway sources, and research articles (Supplementary Material, Table S1). The OBESITOME consisted of 55 samples that were pooled and run as a full slide on the SOLiD 5500XL (Life Technologies, Carlsbad, CA). Color space reads were mapped and aligned against GRCh37/hg19 reference genome using a custom pipeline based on the BWA software and annotated as described previously (31,32). Mean sample coverage for the entire run of 55 samples on the OBESITOME was 100×, median coverage was 87× and 85% of genomic positions were covered by more than 20 reads. The mean coverage for patient 1 and 2 was 161× and 170×, respectively. The criteria for variant detection coverage were set at 10 unique reads, and a non-stringent cut-off for heterozygote allele calls was set at 25–75%. Variants were filtered against the reference frequencies from the datasets of NCBI dbSNP Build 137 for Human (https://www.ncbi.nlm.nih.gov/SNP, last accessed July 2014), Exome Variant Server (EVS) (http://evs.gs.washington.edu/EVS, last accessed July 2014), 1000Genomes (http://www.1000genomes.org, last accessed July 2014), Genome of the Netherlands (http://www.nlgenome.nl, last accessed July 2014) or our in-house dataset, with novel variants and rare variants less than a 0.5% minor allele frequency threshold retained for further analysis. For each patient, a final variant list was compiled including the location in the genomic sequence of the variant, the amino acid change and prioritized on the conservation score and predicted effect on protein function using prediction programs

(Genomic Evolutionary Rate Profiling, Polyphen2, and Sorting Tolerant From Intolerant). Confirmation and segregation analysis in the family of the selected single nucleotide variants or small insertions and deletions was performed by Sanger sequencing.

Whole exome sequencing and analysis for patient 3 was performed as described by the Deciphering Developmental Disorders (DDD) study (1,2). DNA of patient 3 was extracted from saliva samples and exome capture performed using Agilent Sureselect 55 MB Exome Plus (Agilent Technologies, Santa Clara, CA, USA). Exomes were sequenced on the Illumina HiSeq (Illumina, San Diego, CA, USA) and *de novo* analysis performed using DeNovoGear (33). *De novo* variants were validated using Sanger sequencing.

All variants have been submitted to the Leiden Open Variation Database located at http://databases.lovd.nl/shared/genes/KIDINS220, last accessed April 2016.

KIDINS220 Sanger sequencing in a MOMO cohort and patient cDNA

To determine if variants within *KIDINS220* were causal for MOMO syndrome, the full coding regions and exon-intron boundaries of *KIDINS220* were analyzed in a cohort of 10 MOMO patients by Sanger sequencing.

To evaluate the impact of *KIDINS220* variants on RNA expression on our patients, total RNA was isolated from fibroblasts of patient 1 using TRizol Reagent (ThermofFisher Scientific, Waltham, MA, USA) and converted to cDNA with the High-Capacity cDNA Archive Kit (Life Technologies, Carlsbad, CA, USA). Material from patients 2 and 3 was not available. Sanger sequencing on the full cDNA of patient 1 was performed. Furthermore, Quantitative PCR was performed on cDNA of both patient and control fibroblasts using primers before and after the variant c.4050G > A to evaluate if expression of the mRNA was reduced compared with the control. Primer sequences: 5′-CCTGAAGACCCACGTTTCC-3′/5′-AAGCTGAAGTTGAGTGTGTAG G-3′ and 5′-GCTCAGATGTCCCAGTTAGAAG-3′/5′-CTGATGAAC TCTGACCCATGTAATA-3′.

Fibroblast and HEK293 protein preparation and immunoblotting

Fibroblasts of patient 1 and control samples were cultured, lysed, and Western blot analysis performed on the total protein using an antibody recognizing the N-terminus of KIDINS220 (34). Fibroblasts of patient 1 and control samples were cultured according to standard conditions. Frozen cell pellets were lysed at 4 °C in 50mM Tris-HCl pH 7.5, 150 mM NaCl, 1% Triton, 1% Na-deoxycholate, 0.1% SDS and 2 mM EDTA pH8.0 in the presence of protease inhibitors (cOmplete, Roche, Basel, Switzerland) and phosphatase inhibitors (PhosSTOP, Roche, Basel, Switzerland) for 30 min, and sonicated for 10 s. Samples were spun for 5 min at 13.000 rpm at 4 °C.

Western blot analysis was then performed on the total protein extract of the patient fibroblasts using an antibody recognizing the N-terminus of KIDINS220 (34). The supernatant was diluted in 2× Sample buffer (8% SDS/25% Glycerol/0.05M Tris pH 6.8/200 mM DTT/Bromophenol Blue/H_2O) and separated on 6 or 8% SDS-PAGE gels, followed by blotting onto polyvinylidene difluoride membranes (Biorad, Veenendaal, The Netherlands). Blots were blocked with either 2% bovine serum albumin (BSA)/0.05% Tween/phosphate buffered saline (PBS) and incubated overnight with the KIDINS220 antibody. Blots were washed with 0.05%Tween/PBS for three times 10 min each at room temperature and incubated with the appropriate secondary antibody. After washing three times in 0.05% Tween/PBS and once in PBS, blots were developed with Pierce Enhanced Chemiluminescent Western Blotting Substrate (Life Technologies, Carlsbad, CA, USA).

To visualize the molecular weight of the truncated proteins of patients 1 and 2, we introduced the identified point variants in HEK293T cells and performed Western blot analysis on the total protein as described above. HEK293T cells were grown at 37 °C and 5% CO_2 in Dulbecco's Modified Eagle's Medium (DMEM): Ham's F10 nutrient medium (HAMF10) (1:1) medium containing 10% FBS and 1% penicillin/streptomycin. The wild-type *KIDINS220* sequence corresponding to the long isoform of human *KIDINS220* (GenBank accession no. KJ812119) was obtained from an expression construct by using full-length *KIDINS220* primers (primers available upon request) (16). Wild-type *KIDINS220* was ligated into the TOPO entry plasmid pCR8/GW/TOP (Life Technologies BV, Bleiswijk, The Netherlands) and the mutations encoding for Trp1350* and Gln1366* were engineered into the *KIDINS220* expression construct using the QuikChange II XL Site-Directed Mutagenesis Kit (Stratagene, La Jolla, CA, USA) and custom designed primers. The presence of the introduced mutations was confirmed by Sanger sequencing. HEK293T cells were transiently transfected with wild-type and variant DNA constructs using Polyethylenimin (Polyscience, Eppelheim, Germany), grown for 24 h after transfection and prepared and analyzed as described ealier.

Zebrafish expression construct and microinjections in zebrafish embryos

The wild-type *KIDINS220* cDNA sequence or the patient variant Trp1350* were introduced into pCR8/GW/TOPO. The *KIDINS220* middle entry vectors were then used in a multi-site Gateway reaction (ThermoFisher Scientific, Waltham, MA, USA) together with p5E-UAS, p3E-IRES-EGFPpA and as destination vector pDestTol2pA3 (35) to obtain UAS:*KIDINS220* expression vectors. Circular plasmid DNA of UAS:*KIDINS220* constructs was injected at 30 ng/µl in the presence of 25 ng/µl Tol2 mRNA into tg(Isl1BAC:GalFF; UAS:GFP) (14) embryos at the 1-cell stage together with 10 ng/µl pT2ZUASRFP as a fluorescent reporter (36). Healthy embryos displaying robust Isl1-specific RFP fluorescence at 5 dpf was used for spastic activity recordings.

Zebrafish high speed imaging

Embryos at 5 dpf were mounted in 3% methylcellulose (Sigma-Aldrich, Zwijndrecht, The Netherlands) prepared in E3 embryonic medium prior to imaging for 20–60 s with a Hamamatsu C9300-221 high speed CCD camera (Hamamatsu Photonics, Hamamatsu City, Japan) at 82–165 fps mounted on a Leica DM IRBE inverted microscope (Leica Microsystems GmbH, Wetzlar, Germany) at room temperature using Hokawo 2.1 imaging software (Hamamatsu Photonics GmbH, Herrsching am Ammersee, Germany). Image analysis was subsequently carried out with ImageJ (http://rsbweb.nih.gov/ij/, last accessed June 2015). Fischer's exact test was employed to determine significance between Zebrafish groups with different construct injections.

Transfection and immunofluorescence of transfected Neuro2A cells

GW1-MCS expression constructs with a N-terminal HA tag were created with wild-type or p.(Gln1366*) *KIDINS220* inserts. Neuro-2A

cells were seeded at 10 000 cells/cm^2 on poly-L-lysine coated 10 mm coverslips and grown for 24 h in DMEM supplemented in 10% FCS and penicillin/streptomycin. The following day, cells were transfected in DMEM only using Lipofectamine2000 (Thermo Fischer Scientific, Waltham, MA, USA) with N-terminal HA-tagged wild-type or p.(Gln1366*) *KIDINS220* in the GW1-MCS expression vector and cotransfected with a pcDNA/FRT/TO/mCherry expression construct. Cells were incubated for 4 h at 37 °C and 5% CO_2 and medium removed, washed with PBS and replaced with differential medium (DMEM, 1% FCS, 5 uM retinoic acid). Cells were differentiated for 5 days, and differential medium was replaced after 2 and 4 days.

For fixation, medium was removed, the cells were washed once with PBS, and the coverslip treated with 4% PFA (paraformaldehyde) for 15 min at room temperature before being washed again with PBS. Cells were then permeabalized with 0.1% TritonX100 in PBS for 20 min, washed with PBS, blocked in 3% BSA/PBS for 20 min, and washed again. The coverslip was then incubated with 2 ug/ml rabbit Anti-HA-tag antibody Chip Grade in 3% BSA/PBS (ab9110; Abcam, Cambridge, UK) overnight at 4 °C. Coverslips were washed three times in PBS and probed with 1:1000 polyclonal goat anti-rabbit CY5 (Jackson ImmunoResearch, West Grove, PA, USA) in 3% BSA/PBS for 1 h at room temperature. Cells were washed three times in PBS and then stained in 1:5000 DAPI (Thermo Fisher Scientific, Waltham, MA, USA), in 3% BSA/PBS for 15 min, washed three times in PBS, and mounted using Vectashield Antifade Mounting Medium (Vector Laboratories, Burlingame, CA, USA). Coverslips were visualized using a TCS SP8 Confocal Laser Scanning Platform (Leica, Wetzlar, Germany).

Study Approval

Written informed consent from the parents of the all three patients was received prior to inclusion in this study.

Supplementary Material

Supplementary Material is available at *HMG* online.

Acknowledgements

The views expressed in this publication are those of the author(s) and not necessarily those of the Wellcome Trust or the Department of Health. The research team acknowledges the support of the National Institute for Health Research (NIHR), through the Comprehensive Clinical Research Network. P.L.B. is an NIHR Senior Investigator. The DECIPHER database: http://decipher.sanger.ac.uk. We are grateful to the patients and the parents of the patients who agreed to participate in this study.

Conflict of Interest statement: None declared.

Funding

The DDD study presents independent research commissioned by the Health Innovation Challenge Fund (HICF-1009-003), a parallel funding partnership between the Wellcome Trust and the Department of Health, and the Wellcome Trust Sanger Institute (WT098051). The study has UK Research Ethics Committee approval (10/H0305/83, granted by the Cambridge South REC, and GEN/284/12 granted by the Republic of Ireland REC). The research team acknowledges the support of the National Institute for Health Research (NIHR), through the Comprehensive Clinical Research Network.

References

1. The Deciphering Developmental Disorders. (2015) Large-scale discovery of novel genetic causes of developmental disorders. *Nature*, **519**, 223–228.
2. Wright, C.F., Fitzgerald, T.W., Jones, W.D., Clayton, S., McRae, J.F., van Kogelenberg, M., King, D.A., Ambridge, K., Barrett, D.M., Bayzetinova, T., et al. Genetic diagnosis of developmental disorders in the DDD study: a scalable analysis of genome-wide research data. *Lancet*, **385**, 1305–1314.
3. Kong, H., Boulter, J., Weber, J.L., Lai, C. and Chao, M.V. (2001) An evolutionarily conserved transmembrane protein that is a novel downstream target of neurotrophin and ephrin receptors. *J. Neurosci.*, **21**, 176–185.
4. Iglesias, T., Cabrera-Poch, N., Mitchell, M.P., Naven, T.J., Rozengurt, E. and Schiavo, G. (2000) Identification and cloning of Kidins220, a novel neuronal substrate of protein kinase D. *J. Biol. Chem.*, **275**, 40048–40056.
5. Cesca, F., Yabe, A., Spencer-Dene, B., Arrigoni, A., Al-Qatari, M., Henderson, D., Phillips, H., Koltzenburg, M., Benfenati, F. and Schiavo, G. (2011) Kidins220/ARMS is an essential modulator of cardiovascular and nervous system development. *Cell Death Dis.*, **2**, e226.
6. Cesca, F., Yabe, A., Spencer-Dene, B., Scholz-Starke, J., Medrihan, L., Maden, C.H., Gerhardt, H., Orriss, I.R., Baldelli, P., Al-Qatari, M., et al. (2012) Kidins220/ARMS mediates the integration of the neurotrophin and VEGF pathways in the vascular and nervous systems. *Cell Death Differ.*, **19**, 194–208.
7. Wu, S.H., Arevalo, J.C., Sarti, F., Tessarollo, L., Gan, W.B. and Chao, M.V. (2009) Ankyrin Repeat-rich Membrane Spanning/Kidins220 protein regulates dendritic branching and spine stability in vivo. *Dev. Neurobiol.*, **69**, 547–557.
8. Schmieg, N., Thomas, C., Yabe, A., Lynch, D.S., Iglesias, T., Chakravarty, P. and Schiavo, G. (2015) Novel Kidins220/ARMS Splice Isoforms: potential Specific Regulators of Neuronal and Cardiovascular Development. *PLoS One*, **10**, e0129944.
9. Miller, J.N. and Pearce, D.A. (2014) Nonsense-mediated decay in genetic disease: friend or foe? *Mutat. Res. Rev. Mutat. Res.*, **762**, 52–64.
10. White, J., Mazzeu, J.F., Hoischen, A., Jhangiani, S.N., Gambin, T., Alcino, M.C., Penney, S., Saraiva, J.M., Hove, H., Skovby, F., et al. (2015) DVL1 frameshift mutations clustering in the penultimate exon cause autosomal-dominant Robinow syndrome. *Am. J. Hum. Genet.*, **96**, 612–622.
11. Babin, P.J., Goizet, C. and Raldua, D. (2014) Zebrafish models of human motor neuron diseases: advantages and limitations. *Prog. Neurobiol.*, **118**, 36–58.
12. Patten, S.A., Armstrong, G.A., Lissouba, A., Kabashi, E., Parker, J.A. and Drapeau, P. (2014) Fishing for causes and cures of motor neuron disorders. *Dis. Model Mech.*, **7**, 799–809.
13. Halpern, M.E., Rhee, J., Goll, M.G., Akitake, C.M., Parsons, M. and Leach, S.D. (2008) Gal4/UAS transgenic tools and their application to zebrafish. *Zebrafish*, **5**, 97–110.
14. Tessadori, F., van Weerd, J.H., Burkhard, S.B., Verkerk, A.O., de Pater, E., Boukens, B.J., Vink, A., Christoffels, V.M. and Bakkers, J. (2012) Identification and functional characterization of cardiac pacemaker cells in zebrafish. *PLoS One*, **7**, e47644.
15. Arevalo, J.C., Yano, H., Teng, K.K. and Chao, M.V. (2004) A unique pathway for sustained neurotrophin signaling

through an ankyrin-rich membrane-spanning protein. *Embo J.*, **23**, 2358–2368.
16. Bracale, A., Cesca, F., Neubrand, V.E., Newsome, T.P., Way, M. and Schiavo, G. (2007) Kidins220/ARMS is transported by a kinesin-1-based mechanism likely to be involved in neuronal differentiation. *Mol. Biol. Cell*, **18**, 142–152.
17. Lopez-Menendez, C., Gascon, S., Sobrado, M., Vidaurre, O.G., Higuero, A.M., Rodriguez-Pena, A., Iglesias, T. and Diaz-Guerra, M. (2009) Kidins220/ARMS downregulation by excitotoxic activation of NMDARs reveals its involvement in neuronal survival and death pathways. *J. Cell. Sci.*, **122**, 3554–3565.
18. Neubrand, V.E., Cesca, F., Benfenati, F. and Schiavo, G. (2012) Kidins220/ARMS as a functional mediator of multiple receptor signalling pathways. *J. Cell. Sci.*, **125**, 1845–1854.
19. Steinberg, F., Gallon, M., Winfield, M., Thomas, E.C., Bell, A.J., Heesom, K.J., Tavare, J.M. and Cullen, P.J. (2013) A global analysis of SNX27-retromer assembly and cargo specificity reveals a function in glucose and metal ion transport. *Nat. Cell. Biol.*, **15**, 461–471.
20. Andreazzoli, M., Gestri, G., Landi, E., D'Orsi, B., Barilari, M., Iervolino, A., Vitiello, M., Wilson, S.W. and Dente, L. (2012) Kidins220/ARMS interacts with Pdzrn3, a protein containing multiple binding domains. *Biochimie*, **94**, 2054–2057.
21. Marracci, S., Giannini, M., Vitiello, M., Andreazzoli, M. and Dente, L. (2013) Kidins220/ARMS is dynamically expressed during Xenopus laevis development. *Int. J. Dev. Biol.*, **57**, 787–792.
22. Chen, Y., Fu, W.Y., Ip, J.P., Ye, T., Fu, A.K., Chao, M.V. and Ip, N.Y. (2012) Ankyrin repeat-rich membrane spanning protein (kidins220) is required for neurotrophin and ephrin receptor-dependent dendrite development. *J. Neurosci.*, **32**, 8263–8269.
23. Chang, M.S., Arevalo, J.C. and Chao, M.V. (2004) Ternary complex with Trk, p75, and an ankyrin-rich membrane spanning protein. *J. Neurosci. Res.*, **78**, 186–192.
24. Allison, R., Lumb, J.H., Fassier, C., Connell, J.W., Ten Martin, D., Seaman, M.N.J., Hazan, J. and Reid, E. (2013) An ESCRT–spastin interaction promotes fission of recycling tubules from the endosome. *J. Cell Biol.*, **202**, 527–543.
25. Fassier, C., Hutt, J.A., Scholpp, S., Lumsden, A., Giros, B., Nothias, F., Schneider-Maunoury, S., Houart, C. and Hazan, J. (2010) Zebrafish atlastin controls motility and spinal motor axon architecture via inhibition of the BMP pathway. *Nat. Neurosci.*, **13**, 1380–1387.
26. Wood, J.D., Landers, J.A., Bingley, M., McDermott, C.J., Thomas-McArthur, V., Gleadall, L.J., Shaw, P.J. and Cunliffe, V.T. (2006) The microtubule-severing protein Spastin is essential for axon outgrowth in the zebrafish embryo. *Hum. Mol. Genet.*, **15**, 2763–2771.
27. Kernie, S.G., Liebl, D.J. and Parada, L.F. (2000) BDNF regulates eating behavior and locomotor activity in mice. *Embo J.*, **19**, 1290–1300.
28. Liao, G.Y., Li, Y. and Xu, B. (2013) Ablation of TrkB expression in RGS9-2 cells leads to hyperphagic obesity. *Mol. Metab.*, **2**, 491–497.
29. Harakalova, M., Mokry, M., Hrdlickova, B., Renkens, I., Duran, K., van Roekel, H., Lansu, N., van Roosmalen, M., de Bruijn, E., Nijman, I.J., et al. (2011) Multiplexed array-based and in-solution genomic enrichment for flexible and cost-effective targeted next-generation sequencing. *Nat. Protoc.*, **6**, 1870–1886.
30. Monroe, G.R., Harakalova, M., van der Crabben, S.N., Majoor-Krakauer, D., Bertoli-Avella, A.M., Moll, F.L., Oranen, B.I., Dooijes, D., Vink, A., Knoers, N.V., et al. (2015) Familial Ehlers-Danlos syndrome with lethal arterial events caused by a mutation in COL5A1. *Am. J. Med. Genet.*, **167**, 1196–1203.
31. Nijman, I.J., Mokry, M., van Boxtel, R., Toonen, P., de Bruijn, E. and Cuppen, E. (2010) Mutation discovery by targeted genomic enrichment of multiplexed barcoded samples. *Nat. Methods*, **7**, 913–915.
32. Harakalova, M., Nijman, I.J., Medic, J., Mokry, M., Renkens, I., Blankensteijn, J.D., Kloosterman, W., Baas, A.F. and Cuppen, E. (2011) Genomic DNA pooling strategy for next-generation sequencing-based rare variant discovery in abdominal aortic aneurysm regions of interest—challenges and limitations. *J. Cardiovasc. Trans. Res.*, **4**, 271–280.
33. Ramu, A., Noordam, M.J., Schwartz, R.S., Wuster, A., Hurles, M.E., Cartwright, R.A. and Conrad, D.F. (2013) DeNovoGear: de novo indel and point mutation discovery and phasing. *Nat. Methods*, **10**, 985–987.
34. Neubrand, V.E., Thomas, C., Schmidt, S., Debant, A. and Schiavo, G. (2010) Kidins220/ARMS regulates Rac1-dependent neurite outgrowth by direct interaction with the RhoGEF Trio. *J. Cell. Sci.*, **123**, 2111–2123.
35. Kwan, K.M., Fujimoto, E., Grabher, C., Mangum, B.D., Hardy, M.E., Campbell, D.S., Parant, J.M., Yost, H.J., Kanki, J.P. and Chien, C.B. (2007) The Tol2kit: a multisite gateway-based construction kit for Tol2 transposon transgenesis constructs. *Dev. Dyn.*, **236**, 3088–3099.
36. Asakawa, K., Suster, M.L., Mizusawa, K., Nagayoshi, S., Kotani, T., Urasaki, A., Kishimoto, Y., Hibi, M. and Kawakami, K. (2008) Genetic dissection of neural circuits by Tol2 transposon-mediated Gal4 gene and enhancer trapping in zebrafish. *Proc. Natl. Acad. Sci. U. S. A.*, **105**, 1255–1260.